A New Traveling Wave Fault Locating Algorithm for Line Current Differential Relays

E. O. Schweitzer, III, A. Guzmán, M. V. Mynam, V. Skendzic, and B. Kasztenny
Schweitzer Engineering Laboratories, Inc.

S. Marx
Bonneville Power Administration

Presented at the
12th International Conference on Developments in Power System Protection
Copenhagen, Denmark
March 31–April 3, 2014

A new traveling wave fault locating algorithm for line current differential relays

E. O. Schweitzer, III, A. Guzmán*, M. V. Mynam*, V. Skendzic*, B. Kasztenny*, S. Marx†*

**Schweitzer Engineering Laboratories, Inc., 2350 NE Hopkins Court, Pullman, WA 99163 USA,*
bogdan_kasztenny@selinc.com
†Bonneville Power Administration, 1350 Lindsay Boulevard, Idaho Falls, ID 83402 USA

Keywords: fault locating, traveling waves, traveling wave fault locator, differentiator smoother.

Abstract

Faults on overhead power lines cause transients that travel at the speed of light and propagate along the line as traveling waves (TWs). This paper presents a new algorithm for TW fault locating suitable for implementation in line current differential relays. The paper presents the new algorithm in detail, including filtering, phase and mode selection, time stamping, and compensation for dispersion. The paper includes a number of actual field cases from a 161 kV transmission line at Bonneville Power Administration.

1 Introduction

Accurate fault locating on transmission lines is of great value to power transmission asset owners and operators. Fault locating as a discipline dates back to the 1940s. Visual inspection methods evolved from road to air patrols and, more recently, to trials with unmanned aerial vehicles. Fault locating using electrical measurements evolved from simple electromechanical devices to microprocessor-based systems integrated with geospatial data.

Impedance-based fault locating uses voltage and current measurements at system frequency (i.e., the sinusoidal quasi-steady-state phasor quantities combined with different assumptions about the power system for better accuracy). Different assumptions lead to a variety of impedance-based methods. For example, the assumption that the fault current at the fault location is in phase with the fault component of the current at the line terminal led to the Takagi method [1]. Observation that the fault current at the fault location is in phase with the negative-sequence current at the line terminal led to the Schweitzer method [2].

Over the years, several different impedance-based methods have been pursued using information from one or both line ends. The method used in [2] was the first fault locating method integrated into protective relays. This integration accelerated deployment of digital fault locating by making it more practical, convenient, and essentially free. All of these impedance-based methods, however, face accuracy limitations, including nonhomogeneity of the transmission line, uncertainty of the line impedance data, mutual coupling, series compensation, variability of the arc resistance during the fault, transients, taps, limited voltage and current data between fault inception and breaker operation, limited accuracy of instrument transformers, and ground potential rise for close-in faults.

As a result, the accuracy of the impedance-based fault locators is in the order of 0.5 to 2 percent. For a 300-kilometer transmission line, a ±1 percent error still leaves a 6-kilometer section to be patrolled (about 20 towers).

Traveling wave (TW) methods use the naturally occurring surges and waves that are generated by the fault. The TW fault locating methods can approach an accuracy of 300 meters, or about one tower span. Bonneville Power Administration (BPA) has been a pioneer in TW fault locating, with the first implementations dating back to the 1940s. Initially, TW fault locating required only a few technologies that were relatively easy to implement. Advancements in the technology, especially high-speed sampling, digital signal processing, satellite-based synchronization, and digital communications, enable further improvements in TW fault locating.

A fault at any point on the voltage wave other than at voltage zero launches a step wave, which propagates in both directions from the fault location, as shown in Fig. 1.

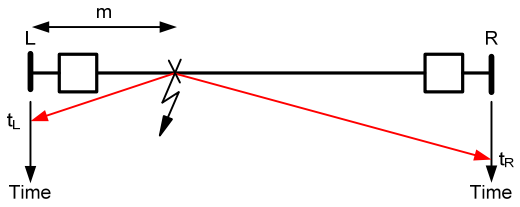

Fig. 1. Fault locating principle of operation using a common time reference.

Modern TW fault locators use a common time reference for the devices capturing the TWs at the line terminals and digital communications to exchange the local time stamps to calculate the distance to fault, *m*, as follows:

$$m = \frac{1}{2}\left[\ell + \left(t_L - t_R\right) \bullet v\right] \quad (1)$$

where:

ℓ is the line length.
t_L is the TW arrival time at L.
t_R is the TW arrival time at R.
v is the TW propagation velocity.

This method leverages the economical and broadly available technologies of digital communications and time synchronization. Most recent digital communications devices can provide absolute time over a wide-area network independent of Global Positioning System (GPS) data [3]. Terrestrial time distribution has the advantage over GPS of being less susceptible to jamming or spoofing.

This paper presents implementation details and field experience of this TW fault locating method recently integrated with microprocessor-based line protection relays [4] [5].

2 Implementation overview

Because the frequency response of current transformers (CTs) is better than for capacitively coupled voltage transformers (CCVTs), we have an immediate preference for using currents for TW fault locating. This may change going forward with the use of better voltage measuring devices.

A convenient implementation is in protective relays, such as line current differential relays and/or distance relays. This aggregation, versus a standalone fault locator, follows on the tremendous acceptance of impedance-based fault locators built into line protection.

The approach taken by our solution is to do the following:

- High-pass filter the currents to eliminate the power system frequency.
- Sample the filter output at a fast rate.
- Eliminate the zero-sequence mode to reduce the effects of dispersion or distortion.
- Determine the instant of arrival of the TWs in a manner consistent and accurate despite the effects due to bandwidth, dispersion, and other factors.
- Communicate the time of arrival from end to end.
- Calculate the fault location.
- Save enough information on every event to back up the results.

We elaborate on these steps in the following sections.

3 Determining the time of arrival

To accurately determine TW arrival time, we begin with a band-pass filter to reject power frequencies, such as 60 Hz and harmonics, and to reject high frequencies to avoid aliasing. The filter step response is shown in Fig. 2. If the TW at the input to the device were an ideal step change, we would measure the signal as shown in Fig. 2.

Real faults, however, generally do not launch ideal steps. Fig. 3 shows a TW current from an actual line fault. It also shows that faults can produce waveforms that make determining the time of arrival a challenge.

Consider using a simple threshold to measure the arrival time. This approach would make the measured arrival time depend on the magnitude, with a potential for error far exceeding several microseconds, as illustrated in Fig. 4.

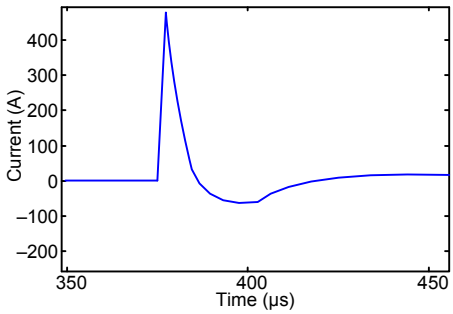

Fig. 2. Step response of the analog filter used to extract TW currents.

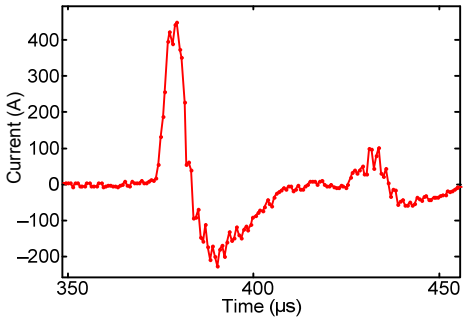

Fig. 3. Sample TW captured at a line terminal during a line fault.

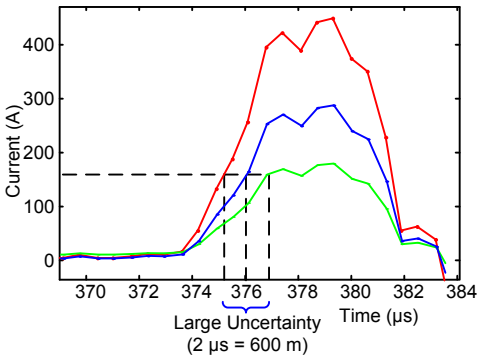

Fig. 4. Using a simple threshold causes considerable arrival time estimation errors.

Consider time-stamping the TW peak. Frequently, however, the wave peak is not well defined. Multiple maxima can be present, produced by ringing in the secondary wires or fast reflections from closely located discontinuities in the primary system (see Fig. 3). In addition, finite sampling rates cause a large time quantization error if we considered the sample of the maximum magnitude as the peak. Filtering, curve-fitting, and interpolation may overcome the latter issue, but the problem of the ill-defined maximum of the current wave will prevent successful implementation of simple peak determination.

Another approach is to time-stamp the TW inception (i.e., the moment at which the TW departs from zero). This can be done by fitting a line into the rising edge of the waveform and calculating the intercept with the time axis. This approach can also be described as calculating the time when the signal is above a certain threshold (see Fig. 4) and correcting it with an

estimate of the time it took the signal to depart from zero and reach the applied threshold.

The problem with this approach is the variance in the TW inception, as shown in Fig. 5. Depending on the portion of the rising edge that is used for fitting the line, we could get considerably different TW arrival time measurements.

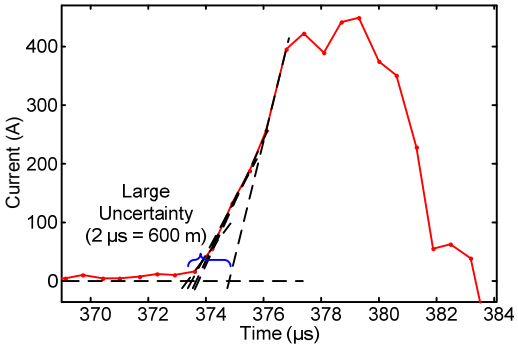

Fig. 5. The estimated inception of the rising edge is impacted by the region selected to fit the line.

Applying extra digital low-pass filtering to smooth the waveform and remove the unwanted distortions does not solve the variance problem of the TW rising edge [5].

Reference [6] describes how this approach has been used in practice. However, there are still better and simpler ways to accurately determine the time of arrival with very small errors from amplitude variations and time quantization.

We determine the arrival time using the differentiator-smoother method. This approach originated in leading edge tracking techniques used in radar [7]. It overcomes most effects of signal distortion and provides excellent interpolation between samples. This method was first used in fault locating in the dc fault locator described in [8] and [9] and is therefore field-proven for the application.

Fig. 6a shows a block diagram suitable for demonstrating the method. The current is first low-pass filtered (or smoothed); then its output is differentiated. Smoothing reduces the effects of waveform distortions and causes the current rising edge to smooth out and become less steep. Softening the rising edge at first may seem contrary to the objective of determining the time of arrival; however, it spreads the edge over several samples, making the time interpolation process possible.

The smoothed waveform is then differentiated, turning the step-like current waveform into a soft pulse-like shape. That pulse-like derivative has its peak at the instant of the steepest slope of the current waveform. The peak of the derivative is relatively insensitive to amplitude changes, being about halfway along the edge, no matter how tall the current step is. Fig. 6c repeats the derivative output and adds the points in time where the samples have been taken. It also shows a pair of lines, and their intersection is an excellent measure of t_a, the arrival time.

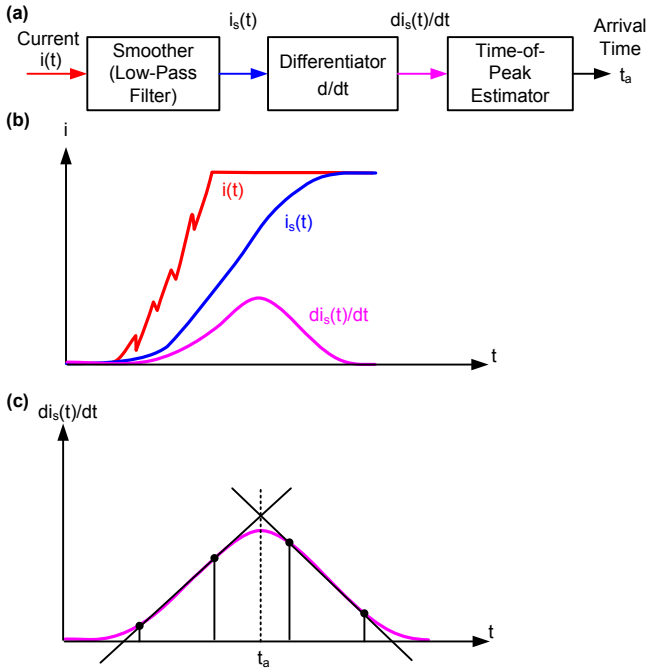

Fig. 6. Differentiator smoother: (a) block diagram, (b) typical waveforms, and (c) time-of-peak estimation.

When using general filters to smooth the derivative of the current, the output resembles a parabola, as shown in Fig. 6b and Fig. 6c. Therefore, in our implementation, we use a parabola-based interpolation method for calculating the arrival time. The algorithm selects a few samples prior to the peak sample and a few samples following the peak. It further uses the least-squares estimation (LSE) method to fit a parabola to the selected points, including the maximum sample, and calculates the arrival time, t_a, using the best-fit parabola (see Fig. 7).

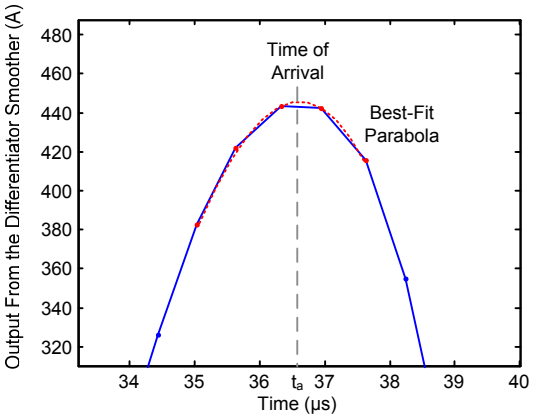

Fig. 7. Accurate time-stamping of the TW using the best-fit parabola.

This method is simple and robust. It provides a time-stamping accuracy better than 0.2 microseconds with our sampling rate of 1.5 MHz.

4 Mode and phase reference selection

To analyze TWs, we use the Clarke transformation [10]. Equation (2) defines the Clarke components of the phase currents with reference to Phase A.

$$\begin{bmatrix} I_0 \\ I_\alpha \\ I_\beta \end{bmatrix} = T_c^{-1} \begin{bmatrix} I_A \\ I_B \\ I_C \end{bmatrix} = \frac{1}{3} \begin{bmatrix} 1 & 1 & 1 \\ 2 & -1 & -1 \\ 0 & \sqrt{3} & -\sqrt{3} \end{bmatrix} \begin{bmatrix} I_A \\ I_B \\ I_C \end{bmatrix} \quad (2)$$

The three modes are referred to as zero sequence, alpha, and beta. If equal currents flow down the Phase A, B, and C conductors and return in the earth, then only the zero-sequence mode, shown in the top row of (2), is excited. If all of the current flows down Phase A and half returns on Phases B and C, then only the alpha mode, shown in the middle row of (2), is excited. If all current flows down Phase B and returns on Phase C, then only the beta mode is excited.

The Clarke components calculated with reference to Phase A work well for AG and BC faults but will not work optimally for other fault types. Therefore, we calculate two other sets referenced to Phases B and C.

The zero-sequence mode is the least appropriate for TW fault locating because it has more attenuation and dispersion than the aerial alpha and beta modes due to greater losses in the earth than in the conductors. This leaves six aerial Clarke components to work with: alpha and beta, each referenced to Phases A, B, or C. Simulations show that alpha and beta components have the following characteristics:

- The alpha currents are available for all fault types. They provide a reliable quantity to detect TWs.
- The beta currents provide marginally higher signal magnitudes for phase-to-phase faults when the phase-to-phase voltage difference at the fault location is higher than the phase-to-ground voltages of the faulted phases.
- Using the highest of the alpha and beta currents reduces the fault location estimation error, but only marginally and only in some cases.

As a result of our findings, our implementation uses the alpha component with the largest amplitude.

5 Compensation for dispersion

The differentiator-smoother algorithm is immune to the magnitude but is affected by the steepness of the TW rising edge. This algorithm time-stamps the midpoints of the rising edges at each terminal, resulting in two different time-stamping errors, e_1 and e_2, as shown in Fig. 8.

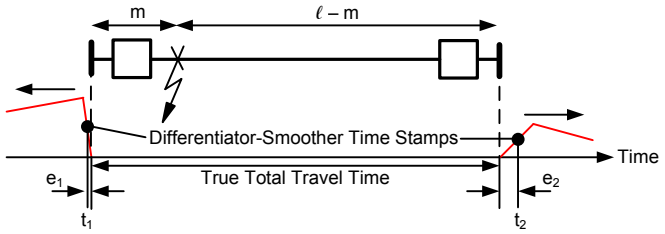

Fig. 8. Dispersion causes different time-stamping errors at the line terminals.

Referring to Fig. 8, we write (3) and (4), where *v* is the actual propagation velocity.

$$t_1 = \frac{m}{v} + e_1 \quad (3)$$

$$t_2 = \frac{\ell - m}{v} + e_2 \quad (4)$$

Assuming the dispersion time-stamping errors are proportional to the traveled distance, *m*, we can write (5) and (6), where *D* is the dispersion per each unit of distance.

$$e_1 = m \bullet D \quad (5)$$

$$e_2 = (\ell - m) \bullet D \quad (6)$$

Substituting (5) and (6) into (3) and (4) and solving for *m,* we obtain:

$$m = \frac{1}{2}\left[\ell + (t_1 - t_2) \bullet \frac{v}{1 + D \bullet v}\right] \quad (7)$$

Observe that (7) is the classic two-end fault locating equation (1) with the propagation velocity adjusted as follows:

$$v_{Used} = \frac{v_{Real}}{1 + D \bullet v_{Real}} \quad (8)$$

The corrected velocity is slightly lower than the actual propagation velocity because $D > 0$.

Measuring the velocity using a line energization test yields a TW propagation velocity that is already corrected for the dispersion effect, assuming the dispersion rate is the same for the entire line length.

6 Field experience

6.1 161 kV transmission line

The Goshen-Drummond 161 kV line is 117.11 kilometers long per the system data book. The line shares a right of way with a 115 kV line for approximately 7.64 kilometers and also

with a 161 kV line for the next 27.36 kilometers. The line was originally built for 115 kV and was later upgraded to 161 kV without initially changing conductors or insulators. BPA has been changing the insulators to the 161 kV rating as they fail or as opportunity arises. The Goshen-Drummond line has 18 sections, with four different tower structures.

After the 161 kV upgrade, the line experienced over 40 faults in 5 years. The most common causes of faults on this line include the following:

- Conductors galloping.
- Farmers spraying fertilizers and inadvertently polluting the conductors and insulators.
- People shooting the conductors and insulators.

6.2 Propagation velocity and line length

Two-end TW fault locating relies on the line length and propagation velocity settings. Refer to (1).

We calculated the propagation velocity using the line length and the measured wave travel time. In order to measure the travel time, we energized the line from the Goshen terminal while the Drummond terminal was open.

We used the time stamps corresponding to pole closing and the reflected TW from the open terminal to calculate the propagation velocity (0.98821 times the speed of light in free space). Being measured with a line energization test, this velocity already considers the effect of dispersion. Refer to (8).

6.3 Power system faults and fault location estimates

Fig. 9 and Fig. 10 show the phase currents captured at the Goshen and Drummond terminals for a CG fault on April 24, 2012.

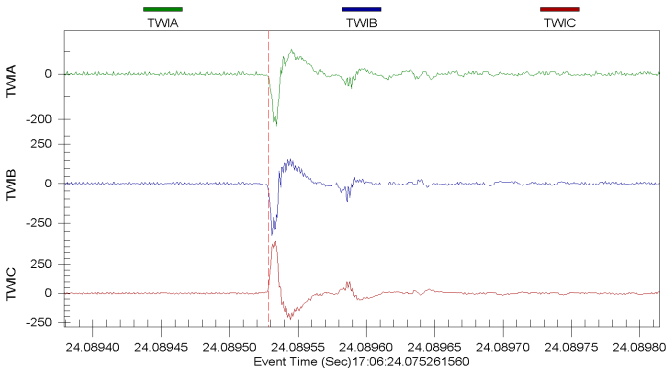

Fig. 9. Phase currents at Goshen for a CG fault at 109.29 kilometers from the Goshen terminal.

Based on the measured TW arrival times, we estimated from (1) a fault location of 109.74 kilometers from the Goshen terminal. When the line crew patrolled the line, they found a damaged insulator at 109.29 kilometers from the Goshen terminal. Fig. 11 shows the damaged insulator. The line crew reported that the cause of the insulator damage was a flashover.

Fig. 12 and Fig. 13 show the phase currents captured at both terminals for a BG fault on June 4, 2013.

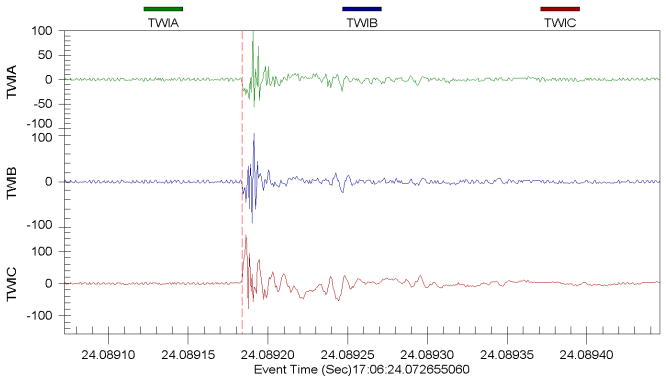

Fig. 10. Phase currents at Drummond for a CG fault at 109.29 kilometers from the Goshen terminal.

Fig. 11. Damaged insulator at 109.29 kilometers from the Goshen terminal.

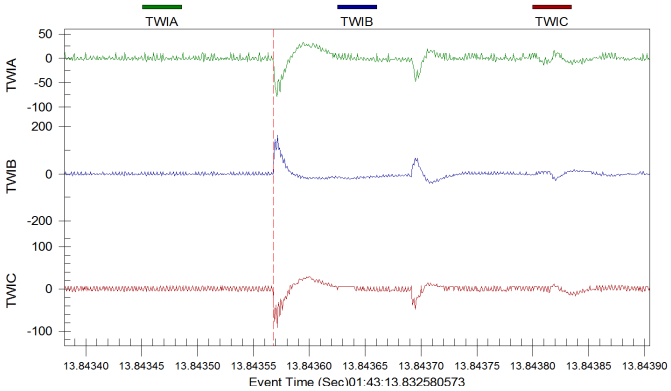

Fig. 12. Phase currents at Goshen for a BG fault at 98.98 kilometers from the Goshen terminal.

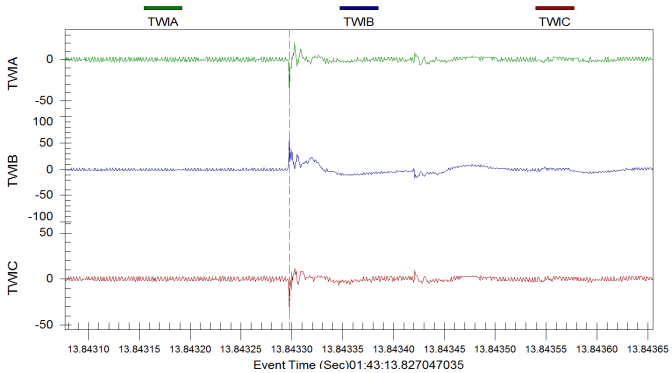

Fig. 13. Phase currents at Drummond for a BG fault at 98.98 kilometers from the Goshen terminal.

We estimated a fault location of 98.85 kilometers from the Goshen terminal. The line crew found the fault at 98.98 kilometers from Goshen. Fig. 14 shows one of the damaged insulators in the insulator string. The line crew reported that the cause of the insulator damage was a flashover.

Fig. 14. Damaged insulator at 98.98 kilometers from the Goshen terminal.

Table 1 provides the fault locations reported by the relay based on TW measurements and the fault locations reported by BPA for a number of faults. The differences between the TW-based estimated distances and the BPA reported distances are attributed to the nonuniformity of the line sag due to terrain elevation changes and differences in tower structures. BPA is working on providing more accurate line length estimates to include line sag.

Date of Event	Faulted Phase	TW Estimated Distance	BPA Reported Distance	Difference
04/24/2012	C	109.74 km	109.29 km	0.45 km
05/11/2012	B	61.12 km	61.41 km	–0.29 km
05/26/2012	B	108.23 km	107.60 km	0.63 km
06/04/2013	B	98.85 km	98.98 km	–0.13 km

Table 1: Reported fault locations and associated differences.

7 Conclusion

TW fault locators built into transmission line protection relays and using standard CTs determine locations of faults to within half a kilometer.

The inherent accuracy of the fault location is better than 0.2 microseconds, or about 60 meters. Thus, the limiting factors may be knowledge of the actual line length and characteristics of the fault.

TW fault locators built into relays add very little cost and eliminate many sources of error found in impedance-based methods.

The authors believe that the improved accuracy, elimination of factors of error, low cost, and ease of use of this new TW fault locating method will contribute substantially to the safe, reliable, and economical operation and maintenance of overhead transmission lines.

References

[1] T. Takagi, Y. Yamakoshi, M. Yamaura, R. Kondow, and T. Matsushima, "Development of a New Type Fault Locator Using the One-Terminal Voltage and Current Data," *IEEE Transactions on Power Apparatus and Systems*, Vol. PAS–101, Issue 8, August 1982, pp. 2892–2898.

[2] E. O. Schweitzer, III, "A Review of Impedance-Based Fault Locating Experience," proceedings of the 15th Annual Western Protective Relay Conference, Spokane, WA, October 1988.

[3] K. Fodero, C. Huntley, and D. Whitehead, "Secure, Wide-Area Time Synchronization," proceedings of the 12th Annual Western Power Delivery Automation Conference, Spokane, WA, April 2010.

[4] S. Marx, B. K. Johnson, A. Guzmán, V. Skendzic, and M. V. Mynam, "Traveling Wave Fault Location in Protective Relays: Design, Testing, and Results," proceedings of the 16th Annual Georgia Tech Fault and Disturbance Analysis Conference, Atlanta, GA, May 2013.

[5] E.O. Schweitzer, III, A. Guzmán, M. V. Mynam, V. Skendzic, B. Kasztenny, and S. Marx, "Locating Faults by the Traveling Waves They Launch," proceedings of the 40th Annual Western Protective Relay Conference, Spokane, WA, October 2013.

[6] M. Aurangzeb, P. A. Crossley, and P. Gale, "Fault Location on a Transmission Line Using High Frequency Travelling Waves Measured at a Single Line End," proceedings of the 2000 IEEE Power Engineering Society Winter Meeting, Singapore, January 2000.

[7] F. E. Nathanson, *Radar Design Principles: Signal Processing and the Environment*. McGraw-Hill Book Co., New York, NY, 1969.

[8] M. Ando, E. O. Schweitzer, III, and R. A. Baker, "Development and Field-Data Evaluation of Single-End Fault Locator for Two-Terminal HVDC Transmission Lines, Part I: Data Collection System and Field Data," *IEEE Transactions on Power Apparatus and Systems*, Vol. PAS–104, Issue 12, December 1985, pp. 3524–3530.

[9] M. Ando, E. O. Schweitzer, III, and R. A. Baker, "Development and Field-Data Evaluation of Single-End Fault Locator for Two-Terminal HVDC Transmission Lines, Part II: Algorithm and Evaluation," *IEEE Transactions on Power Apparatus and Systems*, Vol. PAS–104, Issue 12, December 1985, pp. 3531–3537.

[10] E. Clarke, *Circuit Analysis of A-C Power Systems*. John Wiley & Sons, New York, NY, 1950.

Previously presented at the 12th International Conference on Developments in Power System Protection.